Probing the helium-graphite interaction

Milton W. Cole and D. R. Frankl

Physics Department, The Pennsylvania State University, University Park, Pennsylvania 16802

David L. Goodstein

California Institute of Technology, Pasadena, California 91125

Two separate lines of investigation have recently converged to produce a highly detailed picture of the behavior of helium atoms physisorbed on graphite basal plane surfaces. Atomic beam scattering experiments on single crystals have yielded accurate values for the binding energies of several states for both ^{4}He and ^{3}He, as well as matrix elements of the largest Fourier component of the periodic part of the interaction potential. From these data, a complete three-dimensional description of the potential has been constructed, and the energy band structure of a helium atom moving in this potential calculated. At the same time, accurate thermodynamic measurements were made on submonolayer helium films adsorbed on Grafoil. The binding energy and low-coverage specific heat deduced from these measurements are in excellent agreement with those calculated from the band structures.

CONTENTS

I. INTRODUCTION

As a result of a series of recent developments, the interaction between a helium atom and a graphite surface has become one of the most accurately known properties in surface physics. These developments have included several very different kinds of experiments, as well as a greatly improved theoretical description of the system. The purpose of this article is to review these developments and the picture of the helium-graphite system they have given us.

The basic motivation for interest in this problem derived from the discovery (Thomy and Duval, 1969, 1970; Bretz and Dash, 1971) that exfoliated graphite presents a uniquely homogeneous substrate for studies of physically absorbed monolayer films. In particular, films of ^{3}He and ^{4}He absorbed on a commercial product called Grafoil[1] were found to exhibit a rich variety of phases, transitions, and other phenomena (Bretz *et al.*, 1973; Elgin and Goodstein, 1974; Dash and Schick, 1979). It became a matter of fundamental theoretical importance to sort out which of these phenomena can be ascribed to the behavior of two-dimensional (2D) matter in general, and which are a consequence of the specific helium-graphite interaction.

In 1978, Boato, Cantini, and Tatarek reported measurements of bound-state energies for ^{4}He atoms in the

[1]Union Carbide Corp.

graphite surface potential. These had been deduced from bound-state resonances in atomic beam elastic scattering experiments, using techniques we shall discuss in Sec. II below. They reported that the ground-state energy of the system agreed within a few percent with the zero-temperature binding energy for ^{4}He on Grafoil that had been measured thermodynamically by Elgin and Goodstein (1974).

Using the data of Boato *et al.*, Carlos and Cole (1978) deduced the form of the helium-graphite potential as a function of the distance of the atom from the surface, and used the result to predict bound-state energies for ^{3}He on graphite. Their prediction for the ground-state energy was confirmed in thermodynamic measurements (Elgin, Greif, and Goodstein, 1978) of the $T = 0$ binding energy of ^{3}He on Grafoil. More precise helium-graphite scattering measurements (Derry *et al.*, 1979) and band-structure calculations (Carlos and Cole, 1980b) sharpened the predictions, and brought about even better agreement with the thermodynamic results for both ^{3}He and ^{4}He. The present status of the ground-state energies is shown in Table I.

As we shall see in Sec. II, the atomic beam scattering experiments yielded sufficiently detailed information to permit evaluation of a quantitative helium-graphite potential, not only depending on distance from the surface, but also varying periodically in directions parallel to the basal plane surface. As a result of these periodic lateral variations, a helium atom on a graphite surface has an energy spectrum consisting of

TABLE I. Ground-state energies of He isotopes on basal plane graphite (in meV).

Technique	^{4}He	^{3}He
Scattering [a]	-12.22 ± 0.13	-11.73 ± 0.09
Thermodynamic [b]	-12.27 ± 0.17	-11.72 ± 0.17

[a]Data of Derry *et al.* (1979), as modified by band-structure calculations computed by Carlos and Cole (1980b).
[b]From Elgin and Goodstein (1974) and Elgin, Greif, and Goodstein (1978); the ^{4}He result includes a 2D condensation energy (0.05 meV) calculated by Novaco and Campbell (1975).

     199

2D bands similar to the three-dimensional (3D) energy bands of electrons in metals. The existence of these bands had first been predicted by Dash (1968), and an early attempt to calculate them was made by Hagen, Novaco, and Milford (1972). Their prediction was that the bands are nearly free-particle-like, with only narrow gaps, corresponding to an input potential which varies relatively little across the surface. This was consistent with specific heat data at low coverage (Bretz et al., 1973), which approached the 2D high-temperature limit $C = Nk_B$ for $T \simeq 4$ K (Dash and Schick, 1979). Very recently, however, the scattering data of Boato et al. (1979) and of Derry et al. (1979) have implied that the potential is more corrugated than was previously believed, due to the anisotropic covalent bonding of graphite (Carlos and Cole, 1980a, 1980b). The correspondingly larger band-structure effects are manifested in the specific heat as a deviation from unity in C/Nk_B at higher T (Silva-Moreira, Codona, and Goodstein, 1980).

In Sec. II of this paper, the atomic beam scattering experiments and their interpretation are discussed, together with the determination of the helium-graphite potential and the consequent band structure. In Sec. III we describe the thermodynamic procedures which have yielded measurements of the binding energy for ^{3}He and ^{4}He and confirmed the existence of the bands. The situation is summarized and the significance of these developments for other adsorbates is discussed in Sec. IV.

II. ATOMIC BEAM MEASUREMENTS

A. Diffraction and selective adsorption

In 1929 Estermann and Stern observed the diffraction of a beam of He atoms by a LiF crystal (Estermann and Stern, 1930). This was an important fundamental experiment, since it verified the idea, advanced only four years earlier by de Broglie, that beams of heavy particles possess wave properties.

Current interest in atom diffraction stems from its capability as a surface probe for structural information on the atomic scale. Appropriate wavelengths, of the order of an angstrom, are possessed by low-mass atoms with energies of order 10 meV, as well as by electrons with energies of order 100 eV. Such electrons are only slightly penetrating into solids and are widely used for surface analysis by the technique called LEED (Low-Energy Electron Diffraction; see, for example, Pendry, 1974). Since the atoms are essentially nonpenetrating, they should, in principle, be capable of even higher surface sensitivity. Attempts to develop this capability are now underway in several laboratories around the world. Recent reviews are given by Goodman (1977), Cole and Frankl (1978), and Frankl (1980).

Two kinematic relations governing elastic scattering of particles from a 2D periodic array of scattering centers (viz. a crystal surface) are the Laue equations

$$\mathbf{K}_f = \mathbf{K}_i + \mathbf{G} , \tag{2.1}$$

$$E(K_f) + E_z = \frac{\hbar^2}{2m} k_i^2 . \tag{2.2}$$

Here k_i is the wave vector of the incident beam and $\mathbf{K}_i$

its projection parallel to the surface. $\mathbf{K}_f$ is the corresponding final-state 2D wave vector and $\mathbf{G}$ one of the reciprocal lattice vectors of the surface mesh. Equation (2.1) states the familiar theorem that, in a periodic structure, wave vectors that are congruent modulo reciprocal-lattice vectors are equivalent. Equation (2.2) is simply a statement of energy conservation, $E(K_f)$ and E_z being the energies associated with the parallel and perpendicular parts of the motion in the final state, although in some cases this separation is quite artificial.

Two classes of final states may satisfy these equations.

1. *Free particle states.* For these the separation is valid and

$$E(\mathbf{K}_f) = (\hbar^2/2m)K_f^2 = (\hbar^2/2m)(\mathbf{K}_i + \mathbf{G})^2 . \tag{2.3}$$

Thus solutions exist for all $\mathbf{G}$-vectors leading to positive E_z. i.e., for all $\mathbf{G}$ such that

$$(\mathbf{K}_i + \mathbf{G})^2 \leq k_i^2 . \tag{2.4}$$

Graphically, these are all the $\mathbf{G}$'s lying within a circle of radius k_i centered at $-\mathbf{K}_i$, which is the two-dimensional counterpart of the well known "Ewald sphere" (see, for example, Zachariasen, 1945). They designate the allowed diffraction beams, also called "open channels."

2. *Bound states,* i.e., states in which the particle is held close to the surface by forces of attraction. For such states, E_z is negative. Hence Eq. (2.2) can be satisfied only if $(\mathbf{K}_i + \mathbf{G})^2 > k_i^2$. In other words, the $\mathbf{G}$'s must lie outside the Ewald sphere. All the incident energy plus the binding energy is transformed into $E(K_f)$, the energy of motion parallel to the surface.

In the lowest-order approximation, the latter is treated as free-particle motion in two dimensions, and only then is the separation really valid for bound states. Thus Eq. (2.3) still holds and Eq. (2.2) becomes

$$(\mathbf{K} + \mathbf{G})^2 = k_i^2 - (2m/\hbar^2)E_z = k_i^2 + (2m/\hbar)^2|E_z| . \tag{2.5}$$

This equation describes a circle in the $\mathbf{G}$ plane centered at $-k_i$, or alternatively, a set of circles in the $\mathbf{K}_i$ plane, centered at $-\mathbf{G}$. Since the bound-state energies E_z are discrete, there should be a discrete set of such circles for each $\mathbf{G}$ vector. If they can be identified, their radii yield the corresponding values of $|E_z|$ by Eq. (2.5).

Resonant transitions into such bound states are observed as sharp "anomalies" in the intensities of various elastic beams as functions of the incidence conditions (energy or angles). Such anomalies in the form of localized minima were seen in some of the earliest experiments (Frisch and Stern, 1933), and their identification was proposed by Lennard-Jones and Devonshire (1936, 1937), who gave them the name "selective adsorption." Only in the last few years, however, has a quantitative understanding of the phenomenon begun to emerge. The earlier elastic theories all predicted maxima in the intensity of the (0,0) beam, whereas the earlier experiments gave only minima. Starting with the work of Chow and Thompson in 1976, however, it has become clear that elastic scattering can lead to minima in some cases, maxima in others, and possibly "mini-max" patterns in yet others. In the case of heli-

um scattering from very rigid lattices such as ionic crystals, the agreement of experiment with these scattering theories is very good (Frankl *et al.*, 1978; Harvie and Weare, 1978; Garcia, Celli, and Goodman, 1979).

An important result of the elastic scattering theory was the prediction of slight deviations from the circles of Eq. (2.5). These circles are, as stated above, based on the assumption of free-particle motion (i.e., plane-wave wave functions) in two dimensions. In actuality, the adsorbed atoms move in a two-dimensional periodic potential. Thus their wave functions are Bloch waves (modulated plane waves), and their allowed energies lie in bands separated by gaps. The energy gaps occur at Brillouin-zone boundaries, which correspond to degeneracies of the free-particle states, i.e., intersections of the circles.

The effect can be treated by simple perturbation theory in most cases. If only two states are involved, the wave function is written as a linear superposition of the two zero-order (free-particle) wave functions. As will be discussed in more detail later, first-order degenerate perturbation theory then leads to two K values which deviate from the free-particle circles by amounts related to the matrix element

$$V_{G-G'}^{n,n'} \equiv \int_{-\infty}^{\infty} \phi_n^*(z) V_{G-G'}(z) \phi_{n'}(z) dz ,\qquad (2.6)$$

where $V_G(z)$ is a two-dimensional Fourier component of the periodic potential, and the $\phi_n(z)$ are eigenfunctions of a one-dimensional Schrödinger equation, as discussed below. In regions remote from the intersections the deviations in K are negligible. They become appreciable near the intersections, which are then split into two distinct features, the extent of the splitting being a measure of the magnitude of the corresponding matrix element. One may recognize here a two-dimensional analog of the nearly-free-electron theory of solids. In addition, the surface problem is enriched by the presence of several vibrational states n, so that another kind of degeneracy $(n \neq n')$ can occur.

With this theoretical background, the experimental procedure is as follows.

1. A series of survey scans are made, varying either the polar or the azimuthal angle of incidence, to locate the main features in the specular intensity, and roughly to ascertain their loci in the K plane. An example for ^{4}He graphite is shown in Fig. 1.

2. Working in regions as far as possible from intersections, careful measurements are made to locate the features as precisely as possible. This requires absolute measurement of the angles. The azimuthal angle is no problem, as it can be referenced to an easily identified symmetry direction. The polar angle is, however, very difficult to measure absolutely, owing to the faceted nature of the surfaces. This is especially true of the natural single-crystal graphite flakes needed for these studies. A rather elaborate extrapolation procedure was used to ascertain the true zero of the polar angle in this case (Derry *et al.*, 1979).

3. The measured θ, ϕ, and k values are inserted in Eq. (2.5) to determine the discrete eigenvalues E_n of the energy E_z of perpendicular motion. The G value to be used in each case is determined from the fit of a close-
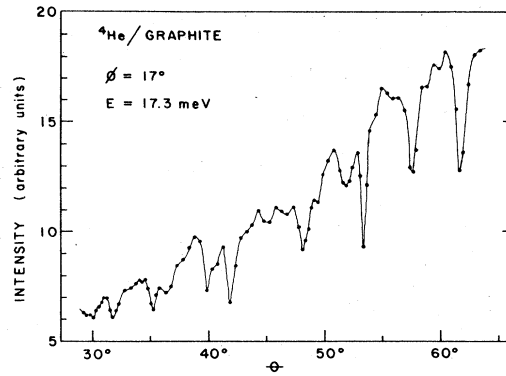

FIG. 1. Specular intensity as function of polar angle. Points are measured values. Lines drawn in only as an aid to the eye. Reprinted from Derry *et al.* (1980).

ly spaced cluster of measured points to a circle. Examples of such determinations are shown in Fig. 2. The results for ^{3}He and ^{4}He on graphite are given in Table II.

4. Turning next to the splittings, sets of closely spaced scans are taken through the regions where simple (i.e., twofold) degeneracies occur. The n, n', G, G' values are determined from the foregoing results and thus values of $|\langle n | V_{G-G} | n'\rangle|$ are obtained. In the case of ^{4}He graphite, the most extensive studies of such splittings have been made by the Genoa group (Boato *et al.*, 1979). Their results are shown in Fig. 3 and listed in Table III. Many of the latter values have been verified under quite different conditions of incidence by the Pennsylvania State group (Derry *et al.*, 1980).

The result of this work is a set of zero-order energy levels and matrix elements of Fourier components of the periodic part of the potential. The use of this information in calculating the properties of absorbed He atoms is described in the next section.

B. Determination of the potential energy

1. Physical origin of the interaction

The ingredients of the helium-graphite interaction are qualitatively similar to those of interatomic potentials (Margenau and Kestner, 1969). At a large separation
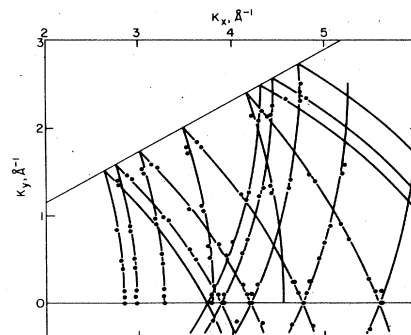

FIG. 2. K-plane loci of specular intensity minima for ^{4}He on graphite at 17.3 meV incident energy. Lines are circles centered at various reciprocal lattice points. Reprinted from Derry *et al.* (1979).

TABLE II. Energy eigenvalues E_n for helium graphite (meV).[a]

n	^{4}He	^{3}He
0	−12.06	−11.62
1	−6.36	−5.38
2	−2.85	−1.78
3	−1.01	
4	−0.17	

[a]Derry et al. (1979). Uncertainties are about ±0.1 meV.

TABLE III. The absolute value of experimental matrix elements $\langle m|V_{10}|n\rangle$ for ^{4}He (meV).[a]

n \ m	0	1	2	3
0	0.28 ± 0.01			
1	0.195 ± 0.015	0.185 ± 0.02		
2	0.125 ± 0.02	0.16 ± 0.015	0.12 ± 0.015	
3	0.09 ± 0.015	0.10 ± 0.01	0.11 ± 0.015	0.08 ± 0.025
4	0.03 ± 0.02			

[a]Boato et al. (1979).

z, $V(\mathbf{r})$ is due to attractive van der Waals forces. For z greater than a few lattice constants, but not so large ($\gtrsim 100$ Å) that retardation is important, its form

$$V(\mathbf{r}) \sim -C_3 z^{-3} \qquad (2.7)$$

can be understood in terms of the interaction between the fluctuating dipole moment of the atom and its image in the substrate. In fact, the expression (MacLachlan, 1964)

$$C_3 = \frac{\hbar}{4\pi} \int \left(\frac{\varepsilon(i\omega) - 1}{\varepsilon(i\omega) + 1} \right) \alpha(i\omega)\, d\omega \qquad (2.8)$$

has the same dependence on dielectric function ε as that for the image of a point charge outside the solid. For the case of graphite, ε is taken to be the geometric mean of the two distinct polarizabilities corresponding to the principal crystallographic directions (Bruch and Watanabe, 1977). Since ε and the He polarizability α are known experimentally, Eq. (2.7) can be evaluated, yielding $C_3 \simeq 186$ meV Å^3 (Vidali, Cole, and Schwartz, 1979). Experimental evidence for this value is discussed in Sec. III.

For closer approach, Eq. (2.7) fails because of the increased role of higher multipole dispersion forces and the commencement of repulsion due to charge overlap. The latter region has been investigated by Free-
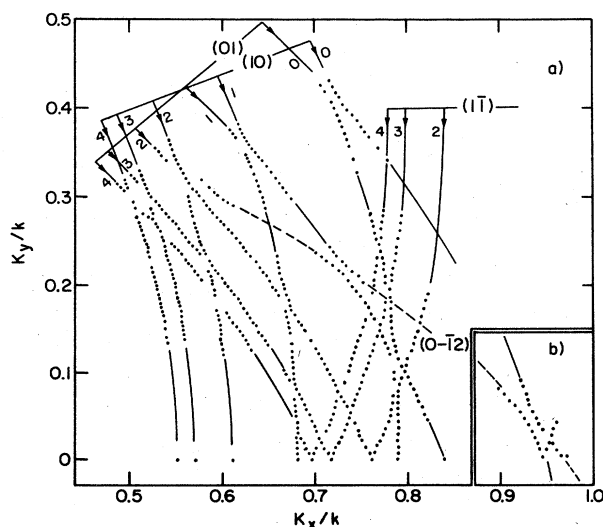

FIG. 3. Detailed behavior of K-plane loci of specular intensity minima in the vicinity of intersections. The incident wavevector magnitude is $k = 6.82$ Å^{-1} ($E = 24.4$ meV) for the insert and 6.49 Å^{-1} ($E = 22.0$ meV) for the main part of the figure. Reprinted from Boato et al. (1979).

man (1975) using the Gordon–Kim version of the density functional method (Gordon and Kim, 1972). As noted by Garcia et al. (1980), the simple procedure of adding Eq. (2.7) to Freeman's potential gives a reasonably accurate representation of $V(\mathbf{r})$; the potential is of approximately the correct depth but is not sufficiently corrugated to account for the matrix elements and diffraction intensities determined by Boato et al. The approximation of simply adding the dispersion term is, in any case, not well justified, although it is fairly common (Landman and Kleiman, 1977; Zaremba and Kohn, 1976, 1977; van Himbergen and Silbey, 1977).

2. Evaluating the interaction potential

An alternative and more conventional approach to deriving the potential assumes that it can be written as a sum of He-C pair interactions:

$$V(\mathbf{r}) = \sum_i U(\mathbf{r} - \mathbf{R}_i), \qquad (2.9)$$

where the sum is over a half-space of C atoms at positions $\mathbf{R}_i$. This is plausible in the absence of screening or other many-body effects (Bennett, 1974). For example, the dispersion contribution to the interatomic potential can be written as $U(x) \sim -C_6 x^{-6}$, where $x = |\mathbf{r} - \mathbf{R}_i|$. For large z, the sum in Eq. (2.9) can be replaced by an integral, yielding Eq. (2.7) with $C_3 = \pi n C_6 / 6$, where n is the number density of atoms in the solid. This agrees with Eq. (2.8) if the Clausius-Mossotti relation is valid and if $n\alpha_{\text{solid}} \ll 1$, which is the condition for negligible screening. For graphite, $n\alpha_{\text{solid}} \simeq 0.3$, indicating that corrections to Eq. (2.9) may be important (Cole, Garrison, and Steele, 1980). Optimistically, one might simply assume the validity of Eq. (2.9), recognizing that U would then be an "effective pair potential." Most efforts to treat this problem have in fact utilized this relation, employing a model pair potential with parameters estimated from "combining rules" (Poshkus, 1965; Steele, 1974). This approach, for example, takes the Lennard-Jones parameter σ to be 2.98 Å, which is the sum of the He radius and one-half the graphite layer spacing. Such assumptions have now been tested by the recent scattering experiments, leading to revisions of our qualitative understanding of $V(\mathbf{r})$.

The first helium-graphite bound-state resonance eigenvalues (Boato et al., 1978) were soon found to be inconsistent with the conventional pair interaction parameters; for example, $\sigma = 2.74$ Å is an optimal choice (Carlos and Cole, 1978) rather than 2.98 Å. Before long

it became evident that a more fundamental assumption is invalid. Specifically $U(x)$ had traditionally been assumed to depend on only the magnitude of x. This is naive, as had been appreciated by Bonino et al. (1975), because the anisotropic bonding and polarizability of the C atoms lead to a rather anisotropic pair interaction. Carlos and Cole (1980a) showed that the scattering data (bound-state eigenvalues of Derry et al., 1979, matrix elements of Boato et al., 1979) are consistent only with pair potentials which incorporate this anisotropy. In particular, since the polarizability perpendicular to the basal plane is small compared to the surface-parallel value, the attractive part of the pair interaction has its minimum magnitude for a given $|x|$ when the He atom is positioned directly above a C atom. By evaluating this anisotropic variation (nearly a factor of two as the angle varies) from the graphite dielectric properties they showed that the net potential $V(r)$ is considerably less smooth than had previously been believed; the site-to-site potential energy barrier (3.6 meV) is more than a factor of 2 larger. Confirmation of this qualitative conclusion comes from a band-structure calculation that does not assume pairwise summation and from thermodynamic data, both of which are described below.

Figure 4 displays the potential energy obtained with the anisotropic 6-12 pair potential by Carlos and Cole (1980a). The probability density ϕ_0^2 shown[2] for ^{4}He corresponds to $\langle z \rangle = 2.92$ Å and $\Delta z_{rms} = 0.25$ Å. Some support for the former value has been obtained from neutron diffraction data by Passell and co-workers (Carneiro et al., 1980). They determined the enhancement of the graphite [002] Bragg peak due to an absorbed He monolayer. The result $\langle z \rangle = (2.85 \pm 0.05)$ Å is
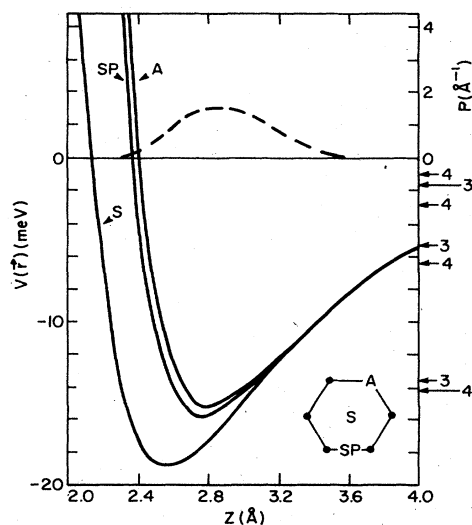

FIG. 4. The full curves are potential energy of an He atom above the graphite symmetry points shown in the lower right corner. The dashed curve is the probability density $\phi_0^2(z)$ for a ^{4}He atom in the laterally averaged potential $V_0(z)$. After Carlos and Cole (1980a). The arrows at the right designate the experimental bound-state resonance energies for ^{3}He and ^{4}He atoms, after Derry et al. (1979).

in favorable agreement with the prediction.[3]

In closing this discussion of potentials, we describe for completeness a series of calculations of the scattering intensity per se. The first efforts (Chow, 1979; Chow and Thompson, 1979) are of only qualitative value because they employed the less accurate isotropic pair potentials. More recently several groups [Garcia et al. (1980); Celli, Garcia, and Hutchison (1979); and Hutchison and Celli (1980)] have used model potentials adjusted to fit the bound-state resonance data. For computational facility, these make the fairly crude assumption that a corrugated hard wall represents the repulsive part of $V(r)$. Nevertheless, they are able to succeed moderately well in characterizing the extant scattering intensity data, including resonance line shapes.

C. Band-structure calculation

An extremely useful aspect of the scattering experiment is that the data can be used quite directly to determine the dispersion relation $E(K)$ for He atoms on graphite (Carlos and Cole, 1980b). The method is formally analogous to that applied to electron bands in solids, but here we have more experimental input available than is customary in that problem.

The basis states for this calculation are eigenfunctions $\phi_n(z)$ of the Schrödinger equation using the laterally averaged potential:

$$V_0(z) = A^{-1} \int d^2R \, V(R, z) \,. \tag{2.10}$$

These eigenfunctions take the form, for a given K,

$$|n, G\rangle = \phi_n(z) \exp[i(K + G) \cdot R] \,. \tag{2.11}$$

The solution for the full potential is a linear combination of such functions, the mixing arising from the periodic part of the potential. Thus

$$\psi(K) = \sum_{n, G} \alpha_{n, G} |n, G\rangle \,; \tag{2.12}$$

and the Schrödinger equation becomes

$$0 = [E_n + \hbar^2(K + G)^2 / 2m - E] \alpha_{n, G} + \sum_{m, G'} \langle n | V_{G-G'} | m \rangle \alpha_{m, G'} \,. \tag{2.13}$$

This can be solved by matrix diagonalization. The E_n values and off-diagonal matrix elements are taken from experimental values of Derry et al. (1979) and Boato et al. (1979). In general, it is necessary to supplement these by values which have not been measured. These can be computed from the ansiotropic 6-12 potential described above. Their inclusion, however, has only a very small effect on the low-energy region of principal interest. The computed dispersion relation, shown in Fig. 5, reveals considerable departure from free-particle character. For example, the direct gap at the Q point of the Brillouin zone is 0.7 meV wide for ^{4}He.

---

[3]It is, in contrast, not consistent with the best fitting Yukawa-6 potential, which has $\langle z \rangle = 2.45$ Å (Carlos and Cole, 1980a), or with the value $\langle z \rangle = 3.25$ Å obtained with the summed 6-12 potential with the parameters used prior to the scattering experiments (Novaco, 1976).
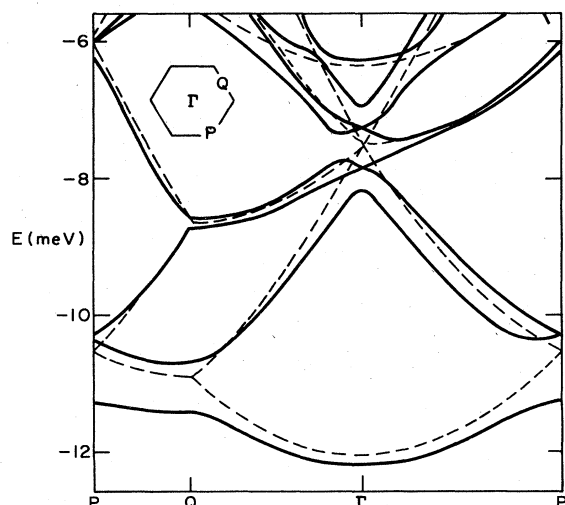
---

[2]A fully three-dimensional calculation (Cole and Toigo, 1980) yields $\langle z \rangle = 2.89$ Å.

FIG. 5. Band structure of ^{4}He on graphite (full curve) for wave vector **K** along symmetry directions in the $2D$ Brillouin zone, shown in the insert. The dashed curve is the corresponding free-particle energy. After Carlos and Cole (1980b).

This amounts to about 70% of the lowest bandwidth, and is more than 50% larger than that calculated with an isotropic pair interaction (Hagen, Novaco, and Milford, 1972). The downward shift of the ground-state energy due to band-structure effects is $E_0 - E_\Gamma = 0.16$ meV (0.11 meV for ^{3}He). While quite small on the scale of the energies themselves, these shifts have been confirmed by thermodynamic measurements summarized in Table I and described below. The smaller band-structure effects for ^{3}He arise from the larger extension of the wave function outward from the corrugated region of the potential.

The density of states per unit area

$$N(E) = A^{-1} \sum_{\nu, \mathbf{K}} \delta [E - E_\nu(\mathbf{K})] , \qquad (2.14)$$

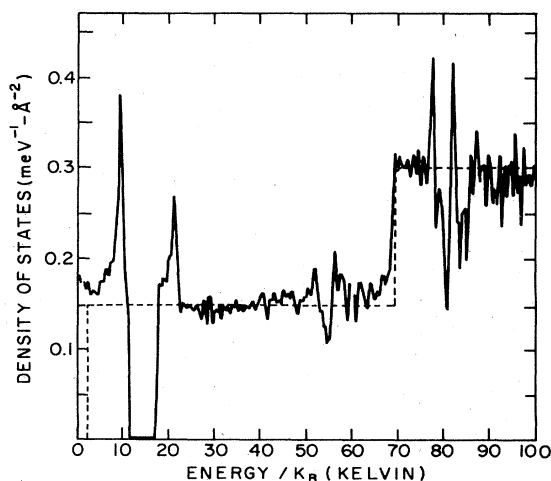where ν is the band index, has been computed from the band structure. Figure 6 compares it with the free-

FIG. 6. Density of states of ^{4}He on graphite (full curve) computed from the band structure. Energies are reckoned from the ground-state energy. The dashed curve is the corresponding free-particle density of states $N_0(E)$ of Eq. (2.16).

particle density of states

$$N_0(E) = (m/2\pi\hbar^2) \sum_n \theta(E - E_n) , \qquad (2.15)$$

which would result in the hypothetical case of a smooth surface (vanishing matrix elements). This function has steps at each E_n due to the excited states of vibration perpendicular to the surface. The most dramatic difference, apart from computational "noise," is the gap evident in $N(E)$. A thermal distribution of particles among these states at temperature T will have a total energy reflecting this difference. A resulting dip in the the classical $2D$ free particle value $C = Nk_B$ has been confirmed in thermodynamic measurements described below.

Also evident in the density of states is a mass enhancement: $m^*/m = 1.06$ for ^{4}He and 1.03 for ^{3}He. There exists a possibility that this enhancement helps to explain the discrepancy between the low-coverage specific heat and the values calculated from a virial expansion (Siddon and Schick, 1974). Other factors which must be incorporated in such a comparison are the averaging of the interaction over motion perpendicular to the surface, and modification of the interparticle interaction by the substrate. While there is strong evidence for such effects, the predicted mass enhancement has not yet been confirmed quantitatively (Vidali and Cole, 1980).

III. THERMODYNAMIC MEASUREMENTS

A. Binding energy

Thermodynamics is a discipline which gives relationships between changes in various properties of a sample as it goes from one state of thermal equilibrium to another. If the sample is a film adsorbed on a solid substrate, the equilibrium properties that can be measured are the temperature T and the pressure P of the vapor in equilibrium with the film. In addition, it is possible to know the number of adsorbate atoms admitted to the system, and, from the volumes and temperature of all parts of the system, to deduce the amount adsorbed, N. One can also measure the amount of heat required to pass from one pressure and temperature to another. From such measurements it has been possible, in the case of helium adsorbed on Grafoil, to find highly accurate values for the binding energy of a single atom to the graphite basal plane at $T = 0$ K, and to demonstrate the existence of energy bands. The purpose of this section is to explain how those results were obtained.

The thermodynamics of physical adsorption has produced a vast literature, both experimental and theoretical (for reviews, see Young and Crowell, 1962, or Steele, 1974). Largely the domain of physical chemists, adsorption techniques were traditionally directed at obtaining two principal parameters: the surface area of a finely divided substrate, and the heat of adsorption for a given adsorbate-substrate system. The surface area may be estimated from a particularly simple kind of measurement, the adsorption isotherm. Heats of adsorption may be measured calorimetrically, or may be deduced from neighboring adsorption isotherms,

much as the heat of vaporization of a liquid may be deduced from its vapor pressure curve using the Clausius-Clapeyron equation. Heats of adsorption are, of course, related to the binding energy of adsorbate to substrate, but the relationship is complicated by thermal effects, and by the fact that most substrates are very far from being homogeneous, or even from being reproducible from one laboratory to another. Nevertheless, attempts have been made by traditional methods to estimate the helium-graphite binding energy. Values of (13.3 ± 0.8) and (11.2 ± 2) meV were found by Grayson and Aston (1957) and Lerner and Daunt (1973), respectively, for ^{4}He.

When the special properties of Grafoil as a substrate were first found (Bretz and Dash, 1971), the quantitatively uncertain situation improved dramatically in a number of ways. For one thing it was found that measurements were highly reproducible in different laboratories (Bretz et al., 1973; Elgin and Goodstein, 1974). For another, a sharp heat capacity peak observed at roughly 3 K and 0.6 layers (in both ^{3}He and ^{4}He) turned out to be due to a lattice-gas ordering transition to a phase having one helium atom occupying every third carbon hexagon in the plane (Bretz et al., 1973). Since the lattice constant of graphite is well known, the ordering peak at the critical coverage N_c affords a means of making a precise evaluation of the surface area of any Grafoil sample. Finally, although the adsorbing surface is not perfectly homogeneous, the number of inhomogeneities is sufficiently small that it seems reasonable to treat them as a perturbation. The behavior of a film on an ideal graphite surface could then be deduced by a kind of iterative thermodynamic modeling procedure (Elgin and Goodstein, 1974). There is one other advantage, not unique to this system but important for the story we are telling: At very low temperature, where there is no desorption, the heat capacity of the graphite substrate becomes so small that the contribution of even a small fraction of a monolayer of helium can be measured.

The result of all of these advantages has been to prompt extensive thermodynamic investigations of submonolayer ^{3}He and ^{4}He films adsorbed on Grafoil by workers at the University of Washington and at Caltech. The Washington data emphasize low-T heat capacities while the Caltech contributions have been vapor pressure data at higher T and N, and combined vapor pressure and heat capacities in a region that overlaps the Washington data. Recently, some thermodynamic data have been presented for helium adsorbed on other graphitized substrates (Bretz, 1977), but in no case other than Grafoil do there exist the extensive and complete data that make possible the kind of analysis to which we are directing attention.

The phases and phase transitions which have excited so much interest in these systems are indicated in Fig. 7, in the form of a specific-heat contour map for ^{4}He on Grafoil. The phenomena which seem particularly well established include a solid phase at high N and low T, bounded by a melting transition which leads to a fluid phase. The fluid phase is, at lower densities, a nearly ideal 2D gas with quantum virial corrections (Siddon and Schick, 1974; Elgin and Goodstein, 1974).
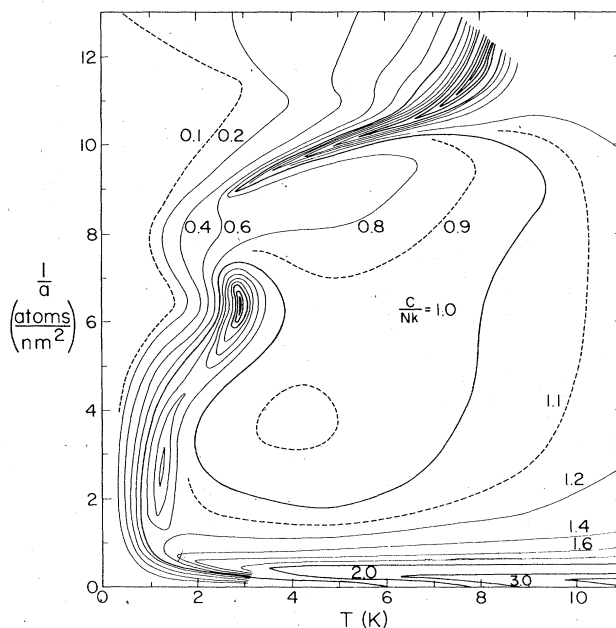

FIG. 7. Contours of constant specific heat for ^{4}He adsorbed on Grafoil, in the density-temperature plane. Heavier lines represent integer values of C/Nk_B. The upper left region corresponds to an incommensurate solid. For $a^{-1} \simeq 6.2$ nm^{-2} and $T \lesssim 3$ K, the atoms form a $\sqrt{3}$ by $\sqrt{3}$ phase in registry with the hexagonal substrate. The second layer starts forming at approximately 11 atoms nm^{-2}. Reprinted from Elgin and Goodstein (1974).

The heat capacity is dominated by the effects of inhomogeneity at very low coverage, and by excitation into higher vibrational states perpendicular to the surface at high temperatures. As noted above, there is also a lattice-gas ordering transition.

It is possible, given data of the kind available for ^{3}He and ^{4}He on Grafoil, to construct complete thermodynamic descriptions of these systems. Such a description consists of a tabulation of an appropriate free energy of the system in terms of its proper variables. Any thermodynamic quantity of interest, e.g., the absolute entropy or the isothermal compressibility, may in principle be deduced from the tabulation if it is sufficiently complete and accurate. A formal description of how the available data may be turned into such a tabulation is given by Elgin and Goodstein (1974). We shall concentrate here on how the quantities of direct interest in this paper are obtained.

At high T and N, vapor pressure measurements give P and T of the 3D gas in the system. The chemical potential of the film, μ, is equal to that of the gas, which is easily deduced from the data since the gas is nearly ideal. Thus for this range of N and T one has obtained in tabular form the function $\mu(T, N)$. From these data alone, one can, for example, find the absolute entropy $S(T, N)$ of the film, provided the data extend to very low N where S necessarily approaches zero.

At lower temperatures, the gas pressure becomes too low to measure directly, but here data are available for the heat capacity at constant coverage, C_N. In addition, there is an overlap region where both vapor

pressure and heat capacities (thermodynamically corrected to eliminate the heat of desorption) are measured. From these data one can construct a table of the absolute entropy by integrating C_N/T at each coverage N:

$$S(T,N) = S(0,N) + \int_0^T \frac{C_N}{T'} dT' . \qquad (3.1)$$

In the case of ^{4}He, comparison of the results of this procedure carried to high T, with the absolute entropy determination from vapor pressure data only, mentioned above, gives $S(0,N) = 0$ for all N, within experimental uncertainty (Elgin and Goodstein, 1974), indicating that the system is indeed in equilibrium. For ^{3}He, the situation is more complicated owing to the nuclear spin degeneracy which is not completely removed at the lowest temperatures studied (roughly 50 mK), but this uncertainty has negligible effect on the results of interest to us here.

From $S(T,N)$, one finds the temperature dependence of μ at each coverage using the Maxwell relation

$$\left(\frac{\partial \mu}{\partial T}\right)_N = -\left(\frac{\partial S}{\partial N}\right)_T . \qquad (3.2)$$

Thus, given values of $\mu(T,N)$ in the vapor pressure region, one may find μ at a lower temperature T_0 and the same N by integrating this equation:

$$\mu(T,N) = \mu(T_0,N) - \int_{T_0}^T \left(\frac{\partial S}{\partial N}\right)_T dT . \qquad (3.3)$$

Having $\mu(T_0,N)$, one can evaluate the equilibrium pressure of the gas when it is far too low to measure by any other means (Taborek and Goodstein, 1979). More importantly for our purposes, in the limit $T_0 \to 0$, we have the quantity

$$\mu(0,N) = \frac{dE(N)}{dN} , \qquad (3.4)$$

where $E(N)$ is the ground-state energy of N atoms on graphite.

Some results of this procedure for ^{3}He on Grafoil are shown in Fig. 8, together with high-temperature values of $\mu(T,N)$ from which $\mu(0,N)$ values are obtained. At very low N, the quantity $-\mu$ is large, due to the presence of activated sites (inhomogeneities) on the surface. However, after the adsorption of just a few percent of a monolayer, $\mu(0,N)$ settles down to a constant value, 136 ± 2 K, the uncertainty being an estimate of the maximum systematic error in the measurement. A plot of $\mu(0,N)$ for ^{4}He on Grafoil over a wider range of N is shown in Fig. 9, where it is compared to values of μ for $3D$ ^{4}He at suitable scaled densities. In the case of ^{4}He, the plateau value of $-\mu(0,N)$ is 143 ± 2 K. The effect of heterogeneity on the low-coverage variation of $\mu(0,N)$ has been evaluated (Elgin and Goodstein, 1974) in terms of a plausible distribution of binding energies. The assumed form leads to the result that the binding energy of the Nth site, starting from the most activated, is

$$E_b(N) = E_\infty[1 + (1 + N/N_0)^{-3}] , \qquad (3.5)$$

where E_∞ is the binding energy on a uniform surface. At 0 K, $-\mu(0,N)$ should correspond closely to $E_b(N)$.
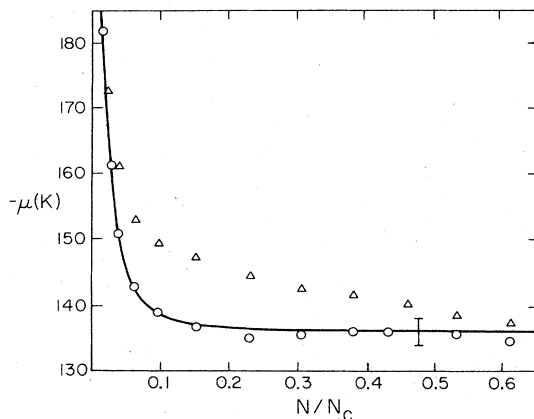
FIG. 8. Chemical potential versus coverage for ^{3}He on Grafoil. N_c is the ordering density, equal roughly to 0.6 layers. Triangles are measured values at $T = 4.18$ K. Circles are thermally corrected to $T = 0$ K, as explained in text. The curve is a plot of Eq. (3.5) with $N_0 = 0.025$ and $E_\infty = 136$. Reprinted from Elgin, Greif, and Goodstein (1978).

The fit in Fig. 8 is obtained by letting $N_0 \simeq 0.025$ layers (N_0 is roughly the number of activated sites) and the factor of 2 binding energy variation as N goes from zero to large values is interpreted as arising from the occasional intersection of two basal plane surfaces.

The quantity of theoretical interest is the binding energy of a single atom on a uniform graphite surface. This differs slightly from $-\mu$ on an ideal surface because the latter includes He-He interactions. In the limit of zero coverage and temperature, the difference equals the binding energy of the $2D$ liquid, which has been calculated for ^{4}He by Novaco and Campbell (1975) to be 0.62 K $= 0.053$ meV. No condensation is predicted for ^{3}He. The ^{4}He correction is incorporated in the binding energy values of Table I. The agreement with the values derived from the empirical band-structure calculation is observed to be excellent.

B. Band-structure effects

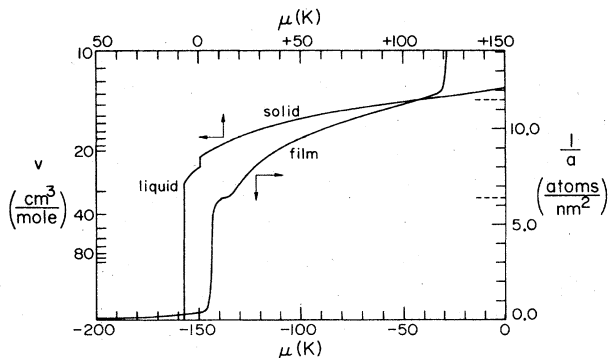We turn now to the way in which the thermodynamic data have been used to ascertain the role of band struc-

FIG. 9. Chemical potential of ^{4}He at $T = 0$ K, for film adsorbed on Grafoil (lower abcissa, right ordinate) and for bulk matter (upper abcissa, left ordinate). Reprinted from Elgin and Goodstein (1974).

ture. An ideal, monatomic gas in two dimensions should have a specific heat given by $C_N/Nk_B = 1$. Prior to the use of Grafoil, various attempts to produce experimental $2D$ matter were deemed unsuccessful because of a failure to find a nearly ideal gas region. In contrast, one of the first dramatic successes of Grafoil was the large flat region, where $C_N/Nk_B \simeq 1$, as may be seen in Fig. 7.

Investigators then set out to examine the departures from $C_N/Nk_B = 1$ in that region. In particular, Siddon and Schick (1974) calculated the quantum-mechanical second virial coefficient for ^{3}He and ^{4}He in two dimensions with interaction parameters taken from $3D$ virial data for the same isotopes. Their results gave a good semiquantitative account of the data, being particularly successful at explaining the differences in departures from ideality in ^{3}He and ^{4}He.

Although clearly on the right track, the theory of Siddon and Schick neglected a number of quantitative effects. One significant consideration is that the low-coverage data to which the theory must be compared is strongly influenced by inhomogeneities. To make a more accurate assessment, Silva-Moreira, Codona, and Goodstein (1980) undertook to correct the data to reveal idea-surface values. Their method makes use of the full data-set available and is based on the distribution of binding sites mentioned above. We shall recount it briefly here.

To simplify the discussion, let us imagine for a moment that the surface consists of regions of two kinds, "ideal" and "activated," where the activated regions simply have a higher binding energy than the ideal regions. In equilibrium, the density of the film on the activated regions will be higher than that on the ideal. The activated portion will thus have a disproportionate fraction of the N atoms in the system, and will contribute a heat capacity characteristic of a higher-density film on an ideal surface at the same temperature. This effect can be corrected iteratively if the chemical potential and heat capacity are known at all N and at neighboring values of T, and if the extent and excess binding energy of the activated region is known.

In fact there is not one kind of activated region, but rather a continuous distribution corresponding to Eq. (3.5). The total heat capacity is the sum of the subsystem heat capacities plus a correction term due to the transfer of atoms between subsystems as the temperature is changed isosterically (i.e., at constant N). Thus (Silva-Moreira et al., 1980)

$$C_N = \left(\frac{\partial E}{\partial T}\right)_N = \sum_i C_{N_i} - T \sum_i \left(\frac{\partial \mu_i}{\partial T}\right)_{N_i} \left(\frac{\partial N_i}{\partial T}\right)_N , \quad (3.6)$$

where the distribution in Eq. (3.5) has been replaced by a large number of discrete subsystems referred to by subscript i. We can solve Eq. (3.6) for C_{N_0} and thereby obtain $C_{N_0}(T, N_0)$, the ideal surface heat capacity, by evaluating all other terms in Eq. (3.6) from the experimental data.

The entire process may be checked by varying the number of subsystems used to simulate Eq. (3.5), and by altering a device used to put an upper limit on the subsystem densities. It is found that the results are insensitive to those changes for coverages above about

0.2 layers. One could presumably do better (i.e., get ideal-surface results at lower coverage) by performing additional iterations of the procedure, but it is sufficient for present purposes to restrict the remaining analysis to results in the region above 0.2 layers.

Once the data have been corrected for inhomogeneities, the next task is to analyze them for quantum virial gas behavior. A $2D$ gas whose departure from ideality may be described by a second virial coefficient, $B(\beta)$, where $\beta = (k_B T)^{-1}$, is expected to have a specific heat given by

$$\frac{C_{N_0}}{N_0 k_B} = 1 - \rho_0 \beta^2 \frac{d^2 B}{d\beta^2} , \quad (3.7)$$

where ρ_0 is the two-dimensional density. The standard analysis consists of plotting $C_{N_0}/N_0 k_B$ versus ρ_0 for each temperature. The results should be a straight line with intercept 1 and slope $\beta^2 d^2 B/d\beta^2$. An example of such a plot is given in Fig. 10.

Silva-Moreira et al., found straight lines, but their intercepts differed systematically from 1 by amounts that were small but outside of experimental uncertainty. These departures from ideality in data already corrected to zero density on a perfect graphite surface are due to the periodic carbon lattice.

In particular, the specific heat of atoms moving in the periodic potential can be evaluated from the band-structure calculation in the limit of very small coverage (Carlos and Cole, 1980b). The result is shown in Fig. 11, where the experimental results are compared to theory. The departure of the predicted C_0 from 1 is due to the density of states in the band structure. As T is raised, C_0 first rises as the excess states below the gap are populated, falls as the gap itself is encountered, then rises again as the states above the gap begin to be filled. This is accompanied by a contribution due to excitation of the second vibrational state of motion perpendicular to the surface. The rise due to promotion above the gap is clearly seen in the ^{4}He data, while the ^{3}He data, which are more complete in the virial gas region, show both the decrease as the gap is encountered and the rise as it is overcome. [L. W. Bruch (preprint, 1981) has done an analytic treatment of band-structure effects in the statistical mechanics.]

C. Thick films

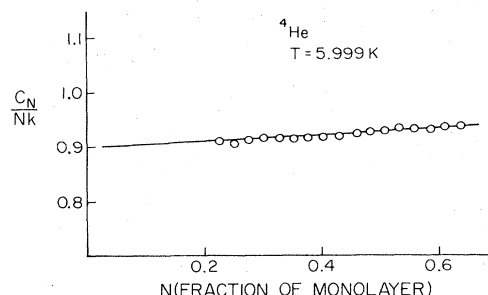Adsorption isotherms for multilayer films can be used to evaluate the coefficient C_3 of the asymptotic

FIG. 10. Virial analysis of specific heat data, ^{4}He on Grafoil, showing intercept differing from $C_N/Nk_B = 1$. Data have been corrected to ideal-surface values as explained in the text.
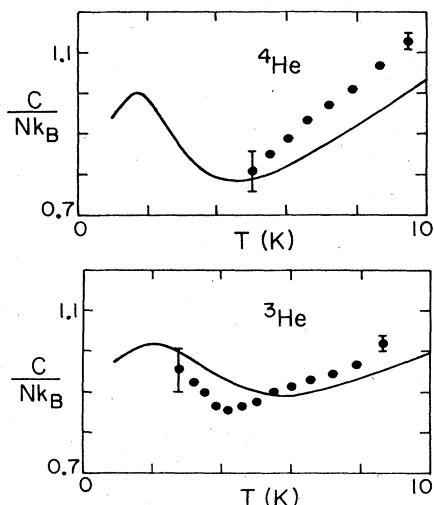
FIG. 11. Specific heats in the limit of zero coverage (the intercepts of plots like Fig. 10) plotted versus temperature and compared to theory, for ^{4}He and ^{3}He on Grafoil. Solid points are intercepts from experimental data, and curves are predictions of band-structure theory.

z^{-3} potential. This procedure entails use of the Frenkel-Halsey-Hill equation, which relates the thickness D to the vapor pressure saturation ratio P/P_0:

$$D = (\Delta C_3/k_B)^{1/3}x , \tag{3.8}$$

where

$$x = [T \ln(P_0/P)]^{-1/3} . \tag{3.9}$$

This result can be derived for thick films by a variety of alternative approximations which are essentially equivalent to the assumption that film growth proceeds by addition of bulk liquid (Steele, 1974 and 1980). The parameter $\Delta C_3 = C_3 - C_3^0$, where $C_3^0 = 10$ meV Å^3, is the coefficient of the van der Waals interaction of the He atom with a hypothetical "substrate" of bulk liquid (Sabisky and Anderson, 1973; Vidali, Cole, and Schwartz, 1979).

A related ansatz is that the total number N of adsorbed atoms includes an excess quantity N_{ex} due to film compression near the substrate. Using Eq. (3.8),

$$N = N_{ex} + nAD = N_{ex} + nA(\Delta C_3/k_B)^{1/3}x , \tag{3.10}$$

where n is the liquid density and A is the surface area. Equation (3.10) can be tested with recent data (Fig. 12) of Bienfait, Dash, and Stoltenberg (1980). For thick films, clustering or capillary condensation causes deviation from Eq. (3.10). A linear dependence on x does occur, however, over an intermediate thickness range (9–18 Å) for four temperatures, the pressure varying by more than an order of magnitude. From the slope and known area (25 m^2) we deduce $\Delta C_3 = (190 \pm 15)$ meV Å^3. This corresponds to a value $C_3 = (200 \pm 15)$ meV Å^3, which is in reasonable agreement with the prediction 186 meV Å^3 of Vidali, Cole, and Schwartz (1979). Similar consistency has been found recently by Roth, Jelatis, and Maynard (1980).

Also of interest is the intercept value of N_{ex}, which yields $N_{ex}/A = 0.092$ Å^{-2}. This is about 0.8 of the monolayer capacity and is in fairly good agreement with re-

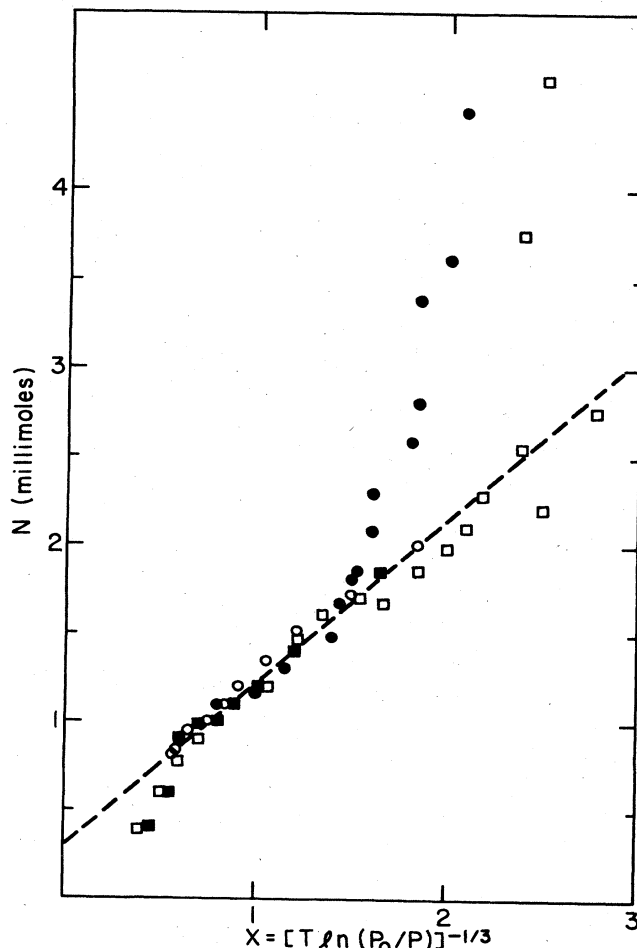FIG. 12. Adsorption isotherms at $T = 1.37$ K (●), $T = 1.55$ K (■), $T = 1.98$ K (□), and $T = 2.539$ K (○) for ^{4}He on graphite foam taken by Bienfait, Dash, and Stoltenberg (1980); a few off-scale points are omitted. The dashed curve corresponds to Eq. (3.10).

cent results of Polanco and Bretz (1980). The latter authors found a ratio 100 : 70 : 64 : 56 for the first four layers, giving an excess equal to 0.66 of the first layer. (Their substrate was the more homogeneous form ZYX graphite, which would plausibly have a smaller value of N_{ex}.) Thus the relation (3.10) is at least semiquantitatively confirmed by these experiments, with plausible values of both N_{ex} and ΔC_3.

IV. FUTURE WORK

Remarkable progress has been made in the last few years toward understanding the helium-graphite interaction. This is due primarily to the comprehensive thermodynamic and scattering measurements described above. It is opportune to address the remaining problems and their prospects for future resolution.

As discussed in Sec. II, the potential derived from summing anisotropic He-C pair interactions works well in fitting the extensive scattering data. Unfortunately, however, a rigorous microscopic theory does not exist. A major obstacle lies in knowing how to merge the overlap repulsion with the dispersion

part; this difficulty is common to the analogous problem of interatomic potentials (Margenau and Kestner, 1969; Ahlrichs, Penco, and Scoles, 1977). The surface problem is exacerbated by our knowing only the leading term ($\sim z^{-3}$) of the dispersion interaction. Further effort in this general area is certainly justified.

On the experimental side, a similar situation prevails. A search by the scattering technique for very weakly bound resonance states can reveal information about the tail of the attractive interaction. The signature of such states is faint, however, because their wave functions extend so far from the surface that they are only weakly coupled to the incident beam. Nevertheless, some success is likely; for example, the $n = 3$ level of ^{3}He should be observable near the predicted value of -0.5 meV.

A worthwhile goal of calorimetric studies is systematic analysis of adsorption on more uniform substrates than Grafoil. This would mitigate the arduous and uncertain task of deconvoluting the effects of heterogeneity.

Other techniques, such as low-energy electron diffraction (Shaw and Fain, 1979), electron appearance potential fine structure (den Boer et al., 1980), and extended x-ray adsorption fine structure (Stern, 1978), have been used recently to probe adsorption. Unfortunately, these are not well suited to the case of He on graphite because of its weak binding and lack of tightly bound electronic core levels. Nevertheless such great strides have been made in this area that one should not be unduly pessimistic.

It is beyond the scope of this paper to describe results for other adsorbates on graphite. Obviously the ideas and techniques discussed here have applications to those cases. For example, the anisotropic pair interaction is also appropriate here and will yield a less smooth potential than has been used to date. In view of forthcoming scattering experiments, we are optimistic about the prospects of comparable success in understanding such problems as have been found for He.

ACKNOWLEDGMENTS

REFERENCES

Ahlrichs, R., R. Penco, and G. Scoles, 1977, Chem. Phys. 19, 119.
Bennett, A. J., 1974, Phys. Rev. B 9, 741.
Bienfait, M., J. G. Dash, and J. Stoltenberg, 1980, Phys. Rev. B 21, 2765.
Boato, G., P. Cantini, and R. Tatarek, 1978, Phys. Rev. Lett. 40, 887.
Boato, G. P., P. Cantini, C. Guidi, R. Tatarek, and G. P. Felcher, 1979, Phys. Rev. B 20, 3957.
Boato, G. P., P. Cantini, R. Tatarek, and G. P. Felcher, 1979, Surf. Sci. 80, 518.
Bonino, G., C. Pisani, F. Ricca, and C. Roetti, 1975, Surf.

Sci. 50, 379.
Bretz, M., 1977, Phys. Rev. Lett. 38, 501.
Bretz, M., and J. G. Dash, 1971, Phys. Rev. Lett. 26, 963.
Bretz, M., J. G. Dash, D. C. Hickernell, E. O. McLean, and O. E. Vilches, 1973, Phys. Rev. A 8, 1589.
Bruch, L. W., 1981, unpublished.
Bruch, L. W., and H. Watanabe, 1977, Surf. Sci. 65, 619.
Carlos, W. E., and M. W. Cole, 1978, Surf. Sci. 77, L173.
Carlos, W. E., and M. W. Cole, 1980a, Surf. Sci. 91, 339.
Carlos, W. E., and M. W. Cole, 1980b, Phys. Rev. B 21, 3713.
Carneiro, K., L. Passell, W. Thomlinson, and H. Taub, 1980, Phys. Rev. B (in press).
Celli, V., N. Garcia, and J. Hutchison, 1979, Surf. Sci. 87, 112.
Chow, H., 1979, Surf. Sci. 79, 157.
Chow, H., and E. D. Thompson, 1976, Surf. Sci. 59, 225.
Chow, H., and E. D. Thompson, 1979, Surf. Sci. 82, 1.
Cole, M. W., and D. R. Frankl, 1978, Surf. Sci. 70, 585.
Cole, M. W., B. Garrison, and W. A. Steele, 1980, (unpublished).
Cole, M. W., and F. Toigo, 1980, submitted to Phys. Rev. B
Dash, J. G., 1968, J. Chem. Phys. 48, 2820.
Dash, J. G., and M. Schick, 1979, in The Physics of Liquid and Solid Helium, edited by K. H. Bennemann and J. B. Ketterson (Wiley, New York), Part 2.
den Boer, M. L., T. L. Einstein, W. T. Elam, R. L. Park, L. D. Roelofs, and G. E. Laramore, 1980, Phys. Rev. Lett. 44, 496.
Derry, G. D., D. Wesner, W. E. Carlos, and D. R. Frankl, 1979, Surf. Sci. 87, 629.
Derry, G. N., D. Wesner, G. Vidali, T. Thwaites, and D. R. Frankl, 1980, Surf. Sci. 94, 221.
Elgin, R. L., and L. Goodstein, 1974, Phys. Rev. A 9, 2657.
Elgin, R. L., J. M. Greif, and D. L. Goodstein, 1978, Phys. Rev. Lett. 41, 1723.
Estermann, I., and O. Stern, 1930, Z. Phys. 61, 95.
Frankl, D. R., 1980, Crit. Rev. Solid State and Mater. Sci. (to be published).
Frankl, D. R., D. Wesner, S. V. Krishnaswamy, G. Derry, and T. O'Gorman, 1978, Phys. Rev. Lett. 41, 60.
Freeman, D. L., 1975, J. Chem. Phys. 62, 941.
Frisch, R., and O. Stern, 1933, Z. Phys. 84, 430.
Garcia, N., W. E. Carlos, M. W. Cole, and V. Celli, 1980, Phys. Rev. B 21, 1636.
Garcia, N., V. Celli, and F. O. Goodman, 1979, Phys. Rev. B 19, 634.
Goodman, F. O., 1977, Crit. Rev. Solid State and Mater. Sci. 7, 33.
Gordon, R. G., and Y. S. Kim, 1972, J. Chem. Phys. 56, 3122.
Grayson, J., and J. G. Aston, 1957, J. Phys. Chem. 61, 610.
Hagen, D. E., A. D. Novaco, and F. J. Milford, 1972, in Adsorption Desorption Phenomena, edited by F. Ricca (Academic, London), p. 99.
Harvie, C. E., and J. H. Weare, 1978, Phys. Rev. Lett. 40, 187.
Hutchison, J., and V. Celli, 1980, Surf. Sci. 93, 263.
Landman, U., and G. G. Kleiman, 1977, in Surface and Defect Properties of Solids, Specialist Report of the Chemical Society, London, Vol. 6, p. 1.
Lennard-Jones, J. E., and A. F. Devonshire, 1936, Nature 137, 1069.
Lennard-Jones, J. E., and A. F. Devonshire, 1937, Proc. R. Soc. London Ser. A 158, 242, 253.
Lerner, E., and J. G. Daunt, 1973, J. Low Temp. Phys. 10, 299.
Margenau, H., and N. R. Kestner, 1969, Theory of Intermolecular Forces (Pergamon, New York).
McLachlan, A. D., 1964, Mol. Phys. 7, 381.
Novaco, A. D., Phys. Rev. B 13, 3194 (1976).
Novaco, A. D., and C. E. Campbell, 1975, Phys. Rev. B 11, 2525.

Pendry, J. B., 1974, *Low Energy Electron Diffraction* (Academic, London).

Polanco, S. E., and M. Bretz, 1980, Surf. Sci. **94**, 1.

Poshkus, D. P., 1965, Discuss. Faraday Soc. **40**, 195.

Roth, J. A., G. J. Jelatis, and J. D. Maynard, 1980, Phys. Rev. Lett. **44**, 333.

Sabisky, E. S., and C. H. Anderson, 1973, Phys. Rev. A **7**, 790.

Shaw, C. G., and S. C. Fain, Jr., 1979, Surf. Sci. **83**, 1.

Siddon, R. L., and M. Schick, 1974, Phys. Rev. A **9**, 907.

Silva-Moreira, A. F., J. Codona, and D. L. Goodstein, 1980, Phys. Lett. A **76**, 324.

Steele, W. A., 1974, *The Interaction of Gases with Solid Surfaces* (Pergamon, Oxford).

Steele, W. A., 1980, Surf. Sci. (in press).

Stern, E. A., 1978, Contemp. Phys. **19**, 289.

Taborek, P., and D. L. Goodstein, 1979, Rev. Sci. Instrum.

50, 227.

Thomy, A., and X. Duval, 1969, J. Chim. Phys. Phys.-Chim. Biol. **66**, 1966.

Thomy, A., and X. Duval, 1970, J. Chim. Phys. Phys.-Chim. Biol. **67**, 286 and 1101.

van Himbergen, J. E., and R. Silbey, 1977, Solid State Commun. **23**, 623.

Vidali, G., M. W. Cole, and C. Schwartz, 1979, Surf. Sci. **87**, L273.

Vidali, G., and M. W. Cole, 1980, Phys. Rev. B **22**, 4661.

Young, D. M., and A. D. Crowell, 1962, *Physical Adsorption of Gases* (Butterworth, London).

Zachariasen, W. H., 1945, *Theory of X-Ray Diffraction in Crystals* (Wiley, New York), p. 85 ff.

Zaremba, E., and W. Kohn, 1976, Phys. Rev. B **13**, 2270.

Zaremba, E., and W. Kohn, 1977, Phys. Rev. B **15**, 1769.